



Study of hydrogen isotopes behavior in tungsten by a multi trapping macroscopic rate equation model

E.A. Hodille, Yves Ferro, Nicolas Fernandez, Charlotte Becquart, Thierry Angot, Jean-Marc Layet, Régis Bisson, Christian Grisolia

► To cite this version:

E.A. Hodille, Yves Ferro, Nicolas Fernandez, Charlotte Becquart, Thierry Angot, et al.. Study of hydrogen isotopes behavior in tungsten by a multi trapping macroscopic rate equation model. *Physica Scripta*, 2016, T167, pp.014011. 10.1088/0031-8949/2016/T167/014011 . hal-01252995

HAL Id: hal-01252995

<https://hal-amu.archives-ouvertes.fr/hal-01252995>

Submitted on 2 Jan 2017

HAL is a multi-disciplinary open access archive for the deposit and dissemination of scientific research documents, whether they are published or not. The documents may come from teaching and research institutions in France or abroad, or from public or private research centers.

L'archive ouverte pluridisciplinaire **HAL**, est destinée au dépôt et à la diffusion de documents scientifiques de niveau recherche, publiés ou non, émanant des établissements d'enseignement et de recherche français ou étrangers, des laboratoires publics ou privés.

Study of Hydrogen Isotopes behavior in tungsten by a multi trapping macroscopic rate equation model

E. A. Hodille^{a,*}, Y. Ferro^b, N. Fernandez^b, C. S. Becquart^c, T. Angot^b, J. M. Layet^b, R. Bisson^b, C. Grisolia^a

^a CEA, IRFM, F-13108 Saint Paul lez Durance, France

^b Aix-Marseille Université, CNRS, PIIM, UMR 7345, 13397 Marseille, France

^c Université Lille I, ENSCL, UMET, UMR 8207, 59655 Villeneuve d'Ascq cedex France

Abstract

Density Functional Theory studies show that in tungsten a mono vacancy can contain up to 6 Hydrogen Isotopes (HIs) at 300K with detrapping energies varying with the number of HIs in the vacancy. Using these predictions, a multi trapping rate equation model has been built and used to model thermal desorption spectrometry (TDS) experiments performed on single crystal tungsten after deuterium ions implantation. Detrapping energies obtained from the model to adjust temperature of TDS spectrum observed experimentally are in good agreement with DFT values within a deviation below 10 %. The desorption spectrum as well as the diffusion of deuterium in the bulk are rationalized in light of the model results.

I. Introduction

To understand the issues of migration, trapping and desorption of Hydrogen Isotopes (HIs) in metals, a Macroscopic Rate Equation (MRE) model is often used. It is based on a one dimensional diffusion equation including trapping effects and was originally discussed by McNabb *et al.* [1]. It has been used for tungsten [2-7] in several codes, such as TMAP7 [5] or our own code MHIMS (Migration of Hydrogen Isotopes in Metals) [7] to fit experimental Thermal Desorption Spectrometry (TDS) measurements. This type of model is based on the assumption that each trap can only contain a single HIs.

However, it has been shown in Density Functional Theory (DFT) studies [8, 9, 10] that a mono vacancy can trap up to 6 HIs at 300 K with detrapping energies depending on the number of HIs

in the vacancy. Inclusion of such effects in a MRE model was recently explored to analyze isotopic exchange experimental observations which are difficult to understand with classical MRE models [11]. In this contribution, a MRE model that includes these DFT predictions is proposed and it is used to probe the impact of HIs multi-trapping on TDS spectra. The implementation of this MRE model is called MHIMS-reservoir. After presenting the basic equation of the model, the code will be used to fit experimental TDS measurements performed on tungsten implanted with HIs ions [12]. Corresponding trapping energies obtained with MHIMS-reservoir will be compared to DFT detrapping energies and the simulation results will permit to discuss the evolution of the filling level of vacancies.

II. Model description

In a 1D MRE model, HIs are split into two populations: mobile (or solute) and trapped species. We will consider a single type of trap (a vacancy for example) which can contain l HIs. In the following, the concentration of HIs and traps, theoretically in m^{-3} , will be normalized to the metal density (i.e. expressed in atomic fraction (at.fr.)). They will be expressed as:

n_{solute}	Concentration of solute sites
C_m	Solute or mobile particles concentration
	Hypothesis 1: $C_m \ll n_{\text{solute}}$ [7]
N_t	Trap concentration. Hypothesis 2: $N_t \ll n_{\text{solute}}$ [7]
N_i	Concentration of traps filled with $i = 0, \dots, l$ HIs, l being the maximum number of HIs that can fill a trap ($l = 6$ in this model)
$C_{t,i} = i \cdot N_i \text{ for } i > 0$	Concentration of trapped HIs

We call a i trap level a trap filled with i HIs. Without trap creation, we get $\forall t, \sum_{i=0}^l N_i = N_t$.

Concerning, the evolution of the trap population, an i trap level can be changed into:

- An $i+1$ trap level by trapping a solute particle (rate $S_{\text{mobile} \rightarrow i \text{ type}}$),
- An $i-1$ trap level by detrapping a trapped particle (rate $S_{i \text{ type} \rightarrow \text{mobile}}$).

As a consequence, the variation of the population N_i of i -trap level can be decomposed in 4 different sources following Eq. (1):

$$\frac{\partial N_i}{\partial t} = -S_{\text{mobile} \rightarrow i \text{ type}} + S_{\text{mobile} \rightarrow i-1 \text{ type}} - S_{i \text{ type} \rightarrow \text{mobile}} + S_{i+1 \text{ type} \rightarrow \text{mobile}} \quad (1)$$

Following hypothesis 2, one can write [7]:

$$S_{mobile \rightarrow i \text{ type}} = \nu_m \cdot \frac{C_m}{n_{solute}} \cdot N_i \quad (2)$$

where ν_m (s^{-1}) is the frequency associated with the trapping process. It can be expressed as a function of the diffusion coefficient by $\nu_m = \frac{D(T)}{\lambda^2}$ and $D(T) = D_0 \cdot e^{-\frac{E_D}{k \cdot T}}$ (m^2/s) is the diffusion coefficient of HIs in the tungsten matrix with E_D the energy barrier for diffusion (eV), T the temperature (K), k the Boltzmann constant and λ is the distance between 2 solute sites.

On the other hand, detrapping processes lead to several associated frequencies ν_i (s^{-1}). The ν_i frequency depends on the temperature and the detrapping energy E_i (eV) of HIs in the i -trap level according to:

$$\nu_i = \nu_0 \cdot e^{-\frac{E_i}{k \cdot T}} \quad (3)$$

with $\nu_0 = 10^{13} s^{-1}$ [3-7] the jump attempt frequency. Following hypothesis 1, one can write:

$$S_{i \text{ type} \rightarrow mobile} = \nu_i \cdot N_i \quad (4)$$

Finally, the variation of trap population $\frac{\partial N_i}{\partial t}$ can be obtained as function of ν_m , ν_i and concentrations:

$$\text{for } 0 < i < l \quad \frac{\partial N_i}{\partial t} = -\nu_m \cdot \frac{C_m}{n_{solute}} \cdot N_i + \nu_m \cdot \frac{C_m}{n_{solute}} \cdot N_{i-1} - \nu_i \cdot N_i + \nu_{i+1} \cdot N_{i+1} \quad (5)$$

$$\text{for } i = 0 \quad \frac{\partial N_0}{\partial t} = -\nu_m \cdot \frac{C_m}{n_{solute}} \cdot N_0 + \nu_1 \cdot N_1 \quad (6)$$

$$\text{for } i = l \quad \frac{\partial N_l}{\partial t} = \nu_m \cdot \frac{C_m}{n_{solute}} \cdot N_{l-1} - \nu_l \cdot N_l \quad (7)$$

This set of equations of the evolution of the trap concentration is based on the same approach as the one described by Schmid *et al.* [11] in the case of mono-isotopic case.

In analogy with a classic MRE model, the variation with time of the concentration of the mobile particles is described in the present model as:

$$\frac{\partial C_m}{\partial t} = D(T) \cdot \frac{\partial^2 C_m}{\partial x^2} - \sum_{i=1}^l \frac{\partial C_{t,i}}{\partial t} + S_{ext} \quad (8)$$

where S_{ext} is the exterior source of particles due to ions implantation expressed as:

$$S_{ext} = (1 - r) \cdot \varphi \cdot f(x) \quad (9)$$

where φ is the incident flux and the TRIM code [13] is used to obtained, the reflexion coefficient r and the stopping range $f(x)$ of the incident ions.

Since $C_{t,i} = i \cdot N_i$ Eq. (8) can be rewritten as:

$$\frac{\partial C_m}{\partial t} = D(T) \cdot \frac{\partial^2 C_m}{\partial x^2} - v_m \cdot \frac{C_m}{n_{solute}} \cdot (N_t - N_l) + \sum_{i=1}^l v_i \cdot N_i + (1 - r) \cdot \varphi \cdot f(x) \quad (10)$$

With Eq. (5), Eq. (6), Eq. (7) and Eq. (10), the model of multi-trapping is fully described. As boundary condition, we consider that it is a Dirichlet one, i.e. $C_m(x = 0, t) = 0$ [7], since recent experimental work [14] has shown that surface processes are not rate-limiting on typical tungsten materials which are not atomically clean.

Finally, we introduce new quantities which allow analyzing mobile particles concentration evolutions in quasi-equilibrium conditions. At the equilibrium $\frac{\partial N_i}{\partial t} = 0$, therefore $N_{eq,i}$ are calculated with the following expression:

$$\text{for } 1 \leq i \leq l \quad \frac{N_{eq,i}}{N_{eq,i-1}} = \frac{v_m \cdot \frac{C_m}{n_{solute}}}{v_i} \quad (11)$$

$$\text{for } 1 \leq i \leq l \quad \frac{N_{eq,i}}{N_{eq,0}} = \frac{(v_m \cdot \frac{C_m}{n_{solute}})^i}{\prod_{j=1}^i v_j} \quad (12)$$

$$\text{for } 0 \leq i \leq l - 1 \quad \frac{N_{eq,l}}{N_{eq,i}} = \frac{(v_m \cdot \frac{C_m}{n_{solute}})^{l-i}}{\prod_{j=1}^{l-i} v_{l-j+1}} \quad (13)$$

And from these we obtained:

$$\sum_{i=0}^l N_{eq,i} = N_t = N_{eq,0} \cdot (1 + \sum_{i=1}^l \frac{(v_m \cdot \frac{C_m}{n_{solute}})^i}{\prod_{j=1}^i v_j}) = N_{eq,l} \cdot (1 + \sum_{i=0}^{l-1} \frac{\prod_{j=1}^{l-i} v_{l-j+1}}{(v_m \cdot \frac{C_m}{n_{solute}})^{l-i}}) \quad (8)$$

So, for a given mobile particles concentration C_m , we are able to calculate each $N_{eq,i}$ which gives, at any time, the trend of evolution of each N_i : if $N_{eq,i} - N_i < 0$, the concentration of N_i tends to decrease to reach the equilibrium and vice versa. By analyzing the concerted evolution of these trap levels concentrations, one is able to extract the global displacement of mobile particles in the material.

MHIMS-reservoir is used here to simulate TDS experiments. To be able to compare the results with experimental data, the code includes 3 stages in the simulation that render the actual measurements, as explained in [7]:

- The implantation stage, lasting t_{imp} at the temperature T_{imp} ,
- The resting stage between the end of the implantation and the beginning of the retention measurement. Here the samples are maintained at constant temperature T_{rest} for a period lasting t_{rest} called the resting time,

- The TDS stage during which the temperature is increased with a given heating ramp β (expressed in $K \cdot s^{-1}$).

III. Model parametrization

In order to test DFT values of HIs detrapping energies in vacancy, we compare the simulations results of MHIMS-reservoir with TDS measurements. In case of polycrystalline tungsten, multiple traps are present such as vacancies, dislocations and grain boundaries. It has been shown by classic MRE models that experiments performed on such materials can be roughly modeled with 2 or 3 traps [2-7]. However, the overlapping of desorption from each kind of trap makes the extraction of information on HIs in vacancies difficult. As a consequence, we chose to model one of the best characterized TDS measurements performed on Single Crystal Tungsten (SCW) by Quastel *et al.* [12]. In these experiments, SCW were mechanically and electrochemically polished with annealing at 1750 K after each polishing step. This procedure should reduce significantly dislocations concentration. Therefore, because there is no grain boundaries in SCW, vacancies are the most probable trapping sites. SCW samples were implanted at room temperature ($T_{imp} = 300 K$) with deuterium at 500 eV/D, at a flux of $10^{20} D \cdot m^{-2} \cdot s^{-1}$ and with a fluence of $10^{23} D \cdot m^{-2}$. Furthermore, Quastel *et al.* [12] have shown that in their ion beam line a LN₂ cold trap allows to reduce the level of volatile impurities. Therefore, we chose to simulate measurements obtained with their LN₂ cold trap and without air exposure before TDS, to avoid impurities effect on D retention. The resting time was indicated to be $t_{rest} = 0.37 h$, the resting temperature was constant ($T_{rest} = 300 K$) and the TDS temperature ramp was $\beta = 5.1 K \cdot s^{-1}$. These parameters were used to feed the following simulations.

In addition, Roszell *et al.* [15] used Nuclear Reaction Analysis (NRA) on the same kind of SCW samples (similar pre-implantation treatment and implantation characteristics 500 eV/D and fluence $\sim 10^{23-24} D \cdot m^{-2}$) to characterize non-homogeneous distribution of implanted D in the bulk of tungsten. As discussed previously in [7], this can be used in first approximation to define the non-homogeneous distribution of vacancies in the materials during implantation. Therefore, we used the D distribution of Roszell *et al.* [15] to define the vacancy trap distribution in our simulation (fig. 1 (a)).

Finally, the diffusion coefficient used in the simulation is the one determined by DFT in [8] $D_H(T) = 1.38 \times 10^{-7} \cdot e^{-\frac{0.2\text{eV}}{k \cdot T}} (m^2 \cdot s^{-1})$. DFT calculations from various authors [8, 9, 10] show that up to $l = 6$ HIs can be trapped in a vacancy at 300 K. Detrapping energies are between 1.5 eV for 1 HIs per vacancy to 0.5 eV for 6 HIs per vacancy. The jump attempt frequency ν_0 calculated by DFT [8] varies in the temperature range of 300 K-1000 K between 0.85×10^{13} and $1.45 \times 10^{13} s^{-1}$. As it remains within the same order of magnitude, the code uses a constant value $\nu_0 = 1 \times 10^{13} s^{-1}$. As a starting point, we used the detrapping energies E_i from Fernandez *et al.* [8] in the MHIMS-reservoir code, before to adjust them in order to minimize the difference between our simulations and the experiment by Quastel *et al.* [12].

IV. Results and discussion

To fit the experimental data and obtain the right hydrogen desorption rate, we consider a distribution of vacancies (fig. 1 (a)) with a high concentration of 10^{-3} at.fr. in the first micrometre. As the formation energy of mono-vacancies in tungsten is above 3 eV [8], these vacancies cannot be thermal vacancies. Remembering that we based our analysis on experiment done on SCW (no grain boundaries) annealed at high temperature (low dislocation concentration), these two potential intrinsic traps cannot be the origin of the high concentration of HIs observed in the first micrometre [15]: trap creation should occur during the implantation even at energies below the displacement threshold. Here we make the assumption that the created traps are vacancies. Indeed, it has been already demonstrated by [17] and classical Molecular Dynamics [18] that HIs induces mono-vacancies formation in tungsten through mechanisms that associated hexagonal self-interstitial clusters and linear crowdion. Moreover, it has also been demonstrated, merging DFT modelling and statistical thermodynamic approach, that at 300 K and at the thermodynamic equilibrium, a solute fraction of $x_{HI} = 10^{-5}$ at.fr. induces a fraction of $\frac{1}{6} \times x_{HI}$ in mono-vacancies filled with $l = 6$ hydrogen atoms [8, 16]. These previous findings support the high vacancy concentration in the sub-surface region as the results of H implantation. The spontaneous formation of vacancies due to hydrogen implantation is not yet present in the model and so to mimic it, a non-homogeneous distribution of vacancies is introduced as explained before.

The resulting simulated TDS spectrum presented in fig. 1 (b) shows 2 desorption peaks at 420 K and 630 K which correspond well with the experimental measurement. It is to note that a change of the spatial distribution of vacancies would change the position of the TDS peak for the same detrapping energies. This is why we based our distribution on experimental NRA measurements [15] to improve the reliability of the model. The final detrapping energies used in this simulation are, from E_6 to E_1 : 0.85 eV, 1.06 eV, 1.17 eV, 1.19 eV, 1.30 eV and 1.31 eV. These energies are in good agreement with DFT values [8-10] (fig. 2), the deviation being below 9% of the starting value from [8]. They are in particular good agreement with DFT results from Fernandez *et al.* [8] where activation energies were calculated from vacancy site to the first nearest neighbour interstitial site and zero point energy corrections were taken into account. Analysis of trap filling levels during the TDS stage allows to interpret the origin of the two desorption peaks. In the following, we note VH_i a vacancy which trapped i HIs. While the first peak is concurrent to the detrapping from VH_6 , the second peak results of the overlapping detrapping from VH_5 to VH_1 .

Now that the MHIMS-reservoir code parametrization is validated by the successful reproduction of TDS measurements, we used the code to interpret the quasi-equilibrium condition that one usually assumes before TDS measurements. Vacancies filling level profiles before the TDS start are presented in fig. 3. Up to a 5 μm depth, vacancies are filled with mainly 5 and 6 HIs (fig. 3 (a)). However, at the edge of this 5 μm depth (fig. 3 (b)), the amount of VH_{5-6} decreases abruptly, concurrently to the increase of, first the VH_4 concentration, then the VH_3 concentration, and so forth until VH_1 are only found in the deepest trapping zone. In this transitioning zone (between 4.5 and 5 μm) where VH_{5-6} left room for VH_{4-1} , the analysis of the $N_{eq,i} - N_i$ quantities (fig. 4) allows to distinguish 2 zones. First, up to 4.7 μm , there is an equilibrium zone with no evolution of the total concentration of particles ($N_{eq,i} - N_i \approx 0$). Then after 4.7 μm , there is the out equilibrium zone where the total concentration of particles drops quickly (fig. 3). Focusing on the 4.7 – 4.8 μm , one notices that the VH_{5-6} concentration tends to increase ($N_{eq,i} - N_i > 0$) while VH_{4-0} concentration tends to decrease ($N_{eq,i} - N_i < 0$). This behavior results from mobile HIs diffusing into this zone containing numerous partly empty traps VH_{4-0} . Mobile HIs are thus “stopped” by being trapped into these VH_{4-0} , forming VH_{5-1} and limiting further HIs migration towards the bulk.

V. Conclusion

In this paper, a rate equation model is presented for multi-trapping/migration of HIs in tungsten having a single type of trap. This model is based on DFT predictions: a mono vacancy can trap up to 6 HIs at 300K. The equations of the model have been described for a general case of a trap which can contain up to l HIs. These equations are implemented in the MHIMS-reservoir code in order to fit experimental TDS measurements obtained on single crystal tungsten in which vacancies are considered to be the most probable trapping site. The simulation results show a good agreement between detrapping energies needed to fit the experimental measurement and the DFT predictions. Two peaks are observed in the TDS spectra at 420 K and 630 K: the first corresponds to desorption of HIs from vacancies filled with 6 HIs and the large second one to the other levels of filling. Studying the equilibrium of equations, a process for the migration at room temperature of HIs in the bulk through vacancies is proposed: mobile particles diffuse through saturated zone and are stopped/trapped where vacancies are not completely filled.

Acknowledgment

This work has been carried out thanks to the support of the A*MIDEX project (n°ANR-11-IDEX-0001-02) funded by the “Investissements d’Avenir” French Government program, managed by the French National Research agency (ANR).

Reference

- [1] McNabb, A., Foster, P. K., Trans. Metall. Soc. AIME, 227 (1963) 618-627
- [2] C. Garcia-Rosales, P. Franzen, H. Planck *et al.*, J. Nucl. Mater. 233-237 (1996) 803-808
- [3] O.V. Ogorodnikova, J. Roth, M. Mayer, J. Nucl. Mater. 313-316 (2003) 469-477
- [4] K. Schmid, V. Rieger, A. Manhard, J. Nucl. Mater. 426 (2012) 247-253
- [5] M. Poon, A. A. Haasz, J. W. Davis, J. Nucl. Mater. 374 (2008) 390-402
- [6] X. Bonnin, E. Hodille, N. Ning *et al.*, J. Nucl. Mater. 463 (2015) 970-973
- [7] E.A. Hodille, X. Bonnin, R. Bisson *et al.*, J. Nucl. Mater. (2015)
<http://dx.doi.org/10.1016/j.jnucmat.2015.06.041>
- [8] N. Fernandez, Y. Ferro, D. Kato, Acta Mater. 94 (2015) 307-318
- [9] K. Heinola, T. Ahlgren, K. Nordlund, J. Keinonen, Phys. Rev. B 82 (2010) 094102
- [10] D.F. Johnson and E.A. Carter, J. Mater. Res. 25 (2010) 315-327
- [11] K. Schmid, U. von Toussaint, T. Schwarz-Selinger, J. Appli. Phys. 116, 134901 (2014)
- [12] A.D. Quastel, J. W. Davis, A.A. Haasz *et al.*, J. Nucl. Mater. 359 (2006) 8-16
- [13] J.F. Ziegler, M.D. Ziegler, J.P. Biersack, Nucl. Inst. Meth. Phys. Res. B 268 (2010) 1818-1823
- [14] R. Bisson, S. Markelj, O. Mourey *et al.*, J. Nucl. Mater. (2015)
<http://dx.doi.org/10.1016/j.jnucmat.2015.07.028>
- [15] J. P. Roszell, J. W. Davis, V. Kh. Alimov *et al.*, J. Nucl. Mater. 438 (2013) S1084-S1087
- [16] K. Ohsawa, F. Nakamori, Y. Hatano *et al.*, J. Nucl. Mater. 458 (2015) 187-197
- [17] S.C. Middleburgh, R.E. Voskoboinikov, M.C. Guenette *et al.*, J. Nucl. Mater. 448 (2014) 270-275
- [18] Y.-N. Liu, T. Ahlgren, L. Bukonte *et al.*, AIP advances 3, 122111 (2013)

Figure Caption

Figure 1. (a) Non-homogeneous vacancy distribution used in this work. (b) Simulations of the TDS spectrum measurement (#15) on a SCW [12] with the non-homogeneous vacancy distribution of (a). Incident ions energy = 500 eV/D, flux = 10^{20} D.m⁻².s⁻¹, fluence 10^{23} D.m⁻², temperature ramp up = 5.1 K/s.

Figure 2. Detrapping energies of HIs in a tungsten mono vacancy as a function of the number of HIs in the vacancy. The detrapping energies are calculated by addition of the DFT binding energies with a barrier for diffusion of the interstitial H equal to 0.2 eV [8-10]. The value $E_{\text{vac-} > \text{solute}}$ correspond to the energy barrier from the vacancy to the first nearest interstitial site [8].

Figure 3. Simulated HIs depth profile just before the TDS start (a) between 0 and 5 μm and (b) between 4.5 and 5 μm (fluence = 10^{23} D.m⁻² with 500 eV/D). $C_{t,1-4}$ are not contributing significantly to retention in (a) and have been removed for clarity

Figure 4. $N_{eq,i} - N_i$ between 4.5 and 5 μm for the mobile profile C_m just before TDS start. $N_{eq,i}$ are calculated using Eq. (5), Eq. (6), Eq. (7) and Eq. (8).

Figure 1

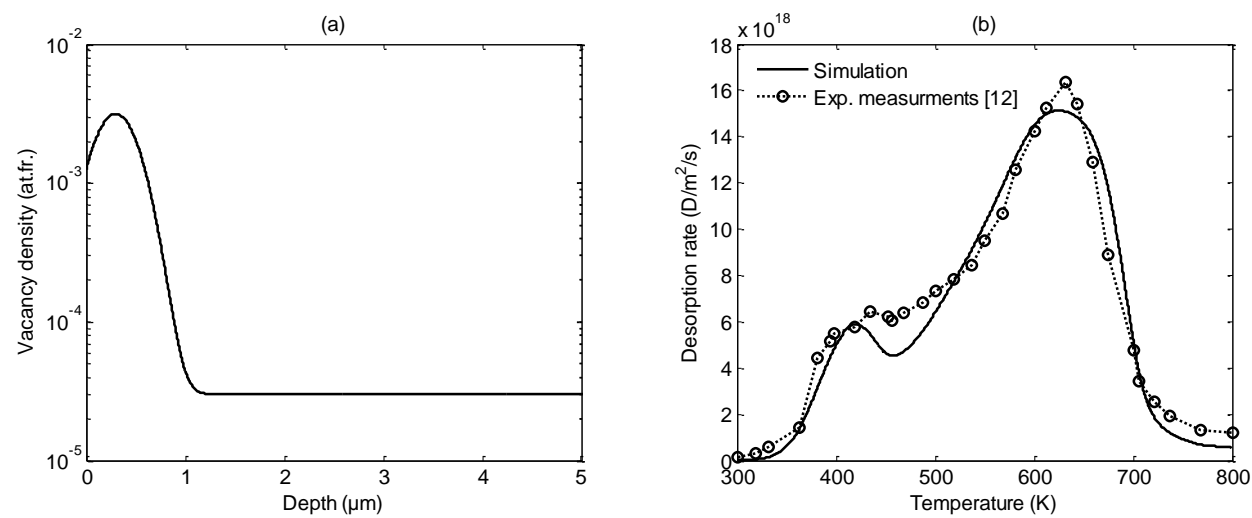


Figure 2

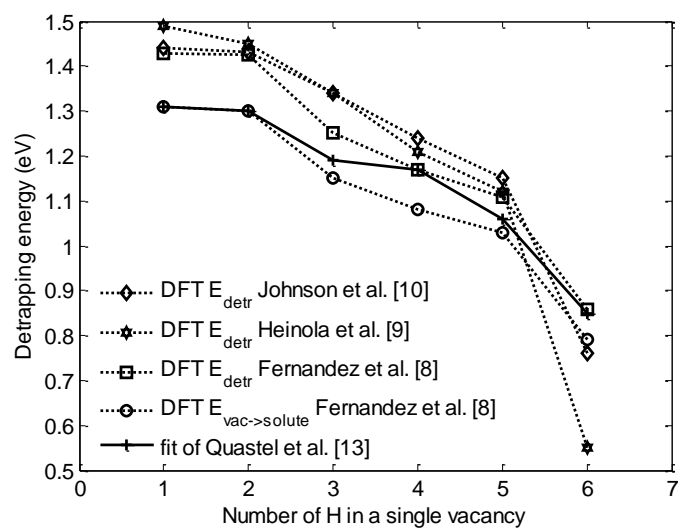


Figure 3

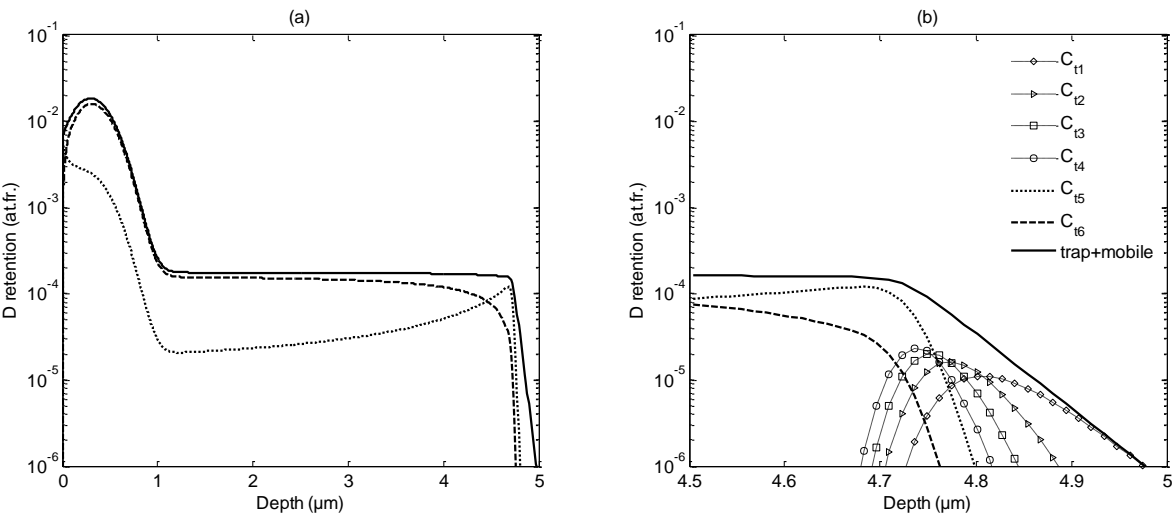


Figure 4

